DEMETER observations of ionospheric heating by powerful VLF transmitters

T.F. Bell, K Graf, U.S. Isnan, D Piddyachiy, Michel Parrot

DEMETER observations of ionospheric heating by powerful VLF transmitters

T. F. Bell,[1] K. Graf,[1] U. S. Inan,[1,2] D. Piddyachiy,[1] and M. Parrot[3]

Received 19 March 2011; revised 27 April 2011; accepted 27 April 2011; published 8 June 2011.

[1] We report DEMETER spacecraft observations of ionospheric heating produced above powerful VLF transmitters by their intense radiated electromagnetic (EM) signals. We compare the heating effects of signals from the 1 MW NWC transmitter in Australia with those produced by signals from the 885 kW NAA transmitter in Maine. Significant observable effects include perturbations in plasma density and thermal electron temperature, and the production of quasi-electrostatic (QE) VLF plasma wave bands, both over the transmitters, and, in the case of NWC, also in the magnetically conjugate region. In the regions in which the QE wave bands were observed, they were invariably accompanied by a band of ELF turbulence with maximum intensity below 300 Hz. Such turbulence has in the past been associated with the presence of small scale plasma density irregularities. This association suggests that heating effects due to NWC are far-reaching and extend along B_o into the conjugate hemisphere where they are expressed in part as small scale plasma density fluctuations. **Citation:** Bell, T. F., K. Graf, U. S. Inan, D. Piddyachiy, and M. Parrot (2011), DEMETER observations of ionospheric heating by powerful VLF transmitters, *Geophys. Res. Lett.*, *38*, L11103, doi:10.1029/2011GL047503.

1. Introduction

[2] Heating of the lower ionosphere by electromagnetic (EM) waves from ground based VLF transmitters was first discussed by *Galejs* [1972], and experimental evidence was first provided by *Inan* [1990] when a VLF analog of the ionospheric cross-modulation effect was observed. *Taranenko et al.* [1992] compared VLF to HF for heating of the lower ionosphere with a focus on ELF generation and found that VLF heating dominates over HF up to ≃90 km altitude. This comparative study was extended by *Barr and Stubbe* [1992]. Work by *Inan et al.* [1992], *Rodriguez and Inan* [1994], and *Rodriguez et al.* [1994] provided additional observations of VLF transmitter heating effects on VLF probe signals, and the results were shown to be consistent with 3-D modeling of the VLF heating and probe signal propagation. *Rodriguez et al.* [1994] further demonstrated that VLF transmitters can cause substantial heating of the overhead nighttime D region on a regular basis.

[3] The first in-situ observations of strong ionospheric perturbations generated by a ground-based VLF transmitter were reported by *Parrot et al.* [2007]. DEMETER spacecraft observations revealed large changes in electron density (N_e) and temperature (T_e) at an altitude of 700 km overhead the powerful VLF transmitter NWC in Australia. *Parrot et al.* [2009] further showed that these perturbed regions allow for increased penetration of MF waves through the ionosphere and, in some cases, a broadband plasma wave enhancement in the VLF range. *Parrot et al.* [2009] suggested that this plasma wave enhancement may be due to either lower attenuation of VLF waves from sferics, or Doppler-shifted narrowband electric fields of the VLF transmitter signal.

[4] In the present paper we review the ionospheric effects produced by the powerful NWC VLF transmitter and compare these effects with those produced by the powerful NAA transmitter in Maine. We then investigate the plasma wave structures that exists in the top-side ionosphere near the conjugate point of the NWC VLF transmitter.

2. Observations

[5] Our data set consists of DEMETER observations on 50 passes over NWC, 50 passes over NAA, and 50 passes over each of the conjugate points of these two transmitters. The passes selected were those which came within 100 km of computed reference points. These points were the positions of the magnetic field lines through each transmitter as the lines intersected 700 km altitude, the approximate altitude of DEMETER, in both hemispheres. Because the DEMETER orbit is sun-synchronous, the local time for all our observations is ≃2230 LT.

2.1. Ionospheric Heating Effects Due to NWC

[6] Figure 1 shows representative DEMETER plasma wave and N_e and T_e observations during a pass over the 1 MW NWC transmitter (21°47′S, 114°09′E) on 22 September 2008, from 1430:30 to 1433:30 UT. Figure 1c shows a 19 to 20 kHz spectrogram of a component of the magnetic (B) field of the NWC signal, as observed by the IMSC instrument [*Parrot*, 2006]. The nominal frequency of the NWC signal is 19.8 kHz, but the bandwidth of the signal is ≃200 Hz at this time as a result of the keying being employed at the transmitter. The signal intensity reaches its maximum during the time interval 1431:00–1432:30 UT. Figures 1d and 1e show N_e and T_e, respectively, as measured by the Langmuir probe instrument (ISL) [*Parrot*, 2006]. N_e decreases by ≃50 % and T_e increases by ≃ 50 % during the time that the wave intensity peaks. These changes in N_e and T_e are attributed to heating of the ionosphere by the NWC VLF signal [*Parrot et al.*, 2007].

[7] Figure 1b shows a 0 to 20 kHz spectrogram of a component of the electric (E) field of plasma waves observed by the ICE instrument [*Parrot*, 2006]. The NWC signal at 19.8 kHz is present at the very top of the spectrogram. In

[1]STAR Laboratory, Stanford University, Stanford, California, USA.
[2]Koc University, Sariyer-Istanbul, Turkey.
[3]LPC2E, CNRS, Orleans, France.

0094-8276/11/2011GL047503

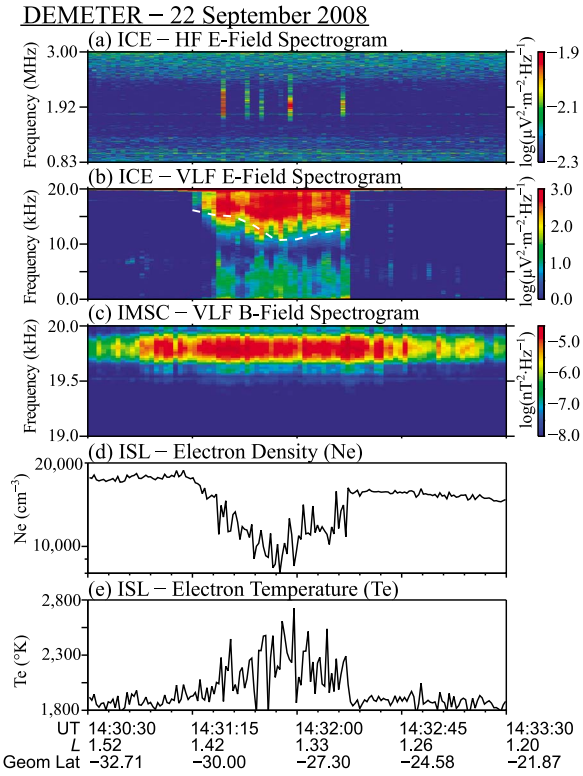

Figure 1. Observations above NWC: (a) spectrogram of impulsive MF signals; (b) spectrogram of an E field component of VLF plasma waves; (c) spectrogram of a B field component of VLF plasma waves; (d) local electron density; (e) local electron temperature. The position of closest approach to the NWC reference point is reached at 1431:33 UT. The magnetic longitude is ≃187°E. DEMETER altitude is ≃668 km.

addition, a band of plasma waves (red color) can be seen which occur only when the spacecraft is located within the heated region where the large perturbations in N_e and T_e are present. This band of plasma waves extends over the approximate frequency range: 12 to 20 kHz, with the lower cutoff frequency approximately equal to the local lower hybrid resonance frequency f_{lhr}. In Figure 1b the calculated value of f_{lhr} is shown by a white dashed line. Since Figure 1c does not show the presence of a B field for the band of plasma waves seen in Figure 1b, it can be assumed that the waves are QE waves rather than EM waves. Thus we refer to this band as the QE wave band.

[8] Figure 1a shows a 0.83 to 3.33 MHz spectrogram including impulsive MF signals observed within the heated region. These signals are believed to be the high frequency portions of impulsive lightning-generated whistlers [*Parrot et al.*, 2009] which are able to penetrate the F region of the ionosphere because of the large perturbations in N_e produced by the NWC transmitter. The observations shown in Figure 1 are similar to those reported by *Parrot et al.* [2007] and *Mishin et al.* [2010]. However, it should be noted that *Mishin et al.* [2010] attributed the MF signals to a local source of electrostatic upper hybrid waves.

2.2. Ionospheric Heating Effects Due to NAA

[9] Figure 2 shows representative DEMETER plasma wave and N_e and T_e observations during a pass over the 885 kW NAA transmitter (44°39′N, 67°17′W) on 15 April 2007, from 0210:15 to 0212:00 UT. Figure 2b shows a 0 to 20 kHz spectrogram of a component of the observed E field of plasma waves. The aliased 24.0 kHz NAA signal appears at 16.0 kHz. Although the 24.0 kHz frequency of NAA is well outside the nominal pass band of the DEMETER VLF receiver (0–20 kHz), the intensity of the NAA signal is high enough that the aliased signal appearing at 16.0 kHz can still be well resolved, in spite of the ≃20 dB loss of intensity imposed by the anti-aliasing filter. In addition to the NWC signal, a band of plasma waves (red color) can be seen which extend over the approximate frequency range 9 to 20 kHz. Since the band of plasma waves exhibits no significant B field, as evidenced in Figure 2c, these waves form a QE wave band. The intensity of the QE wave band in Figure 2b is approximately the same as that in Figure 1b. In Figure 2b the calculated value of f_{lhr} is shown by a white dashed line.

[10] The QE wave band is observed only during the time interval 0210:54–0211:14 UT, coincident with enhanced fluctuations in N_e and T_e as shown in Figure 2d and 2e, respectively. When the QE wave band is first observed, there is an abrupt decrease in N_e of ≃30%, after which N_e slowly increases back towards its original level. It then abruptly decreases at the time at which the QE band disappears. In Figure 2d, a dark line parallel to the time axis marks the period of enhanced fluctuations. Over the same

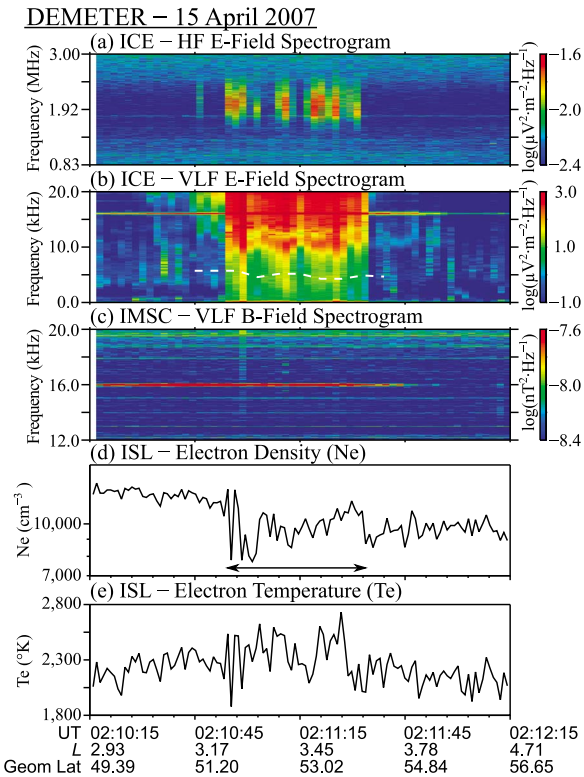

Figure 2. Observations above NAA: (a) spectrogram of impulsive MF signals; (b) spectrogram of an E field component of VLF plasma waves; (c) spectrogram of a B field component of VLF plasma waves; (d) local electron density; (e) local electron temperature. The position of closest approach to the NAA reference point is reached at 0211:15 UT. The magnetic longitude is ≃6°E. DEMETER altitude is ≃668 km.

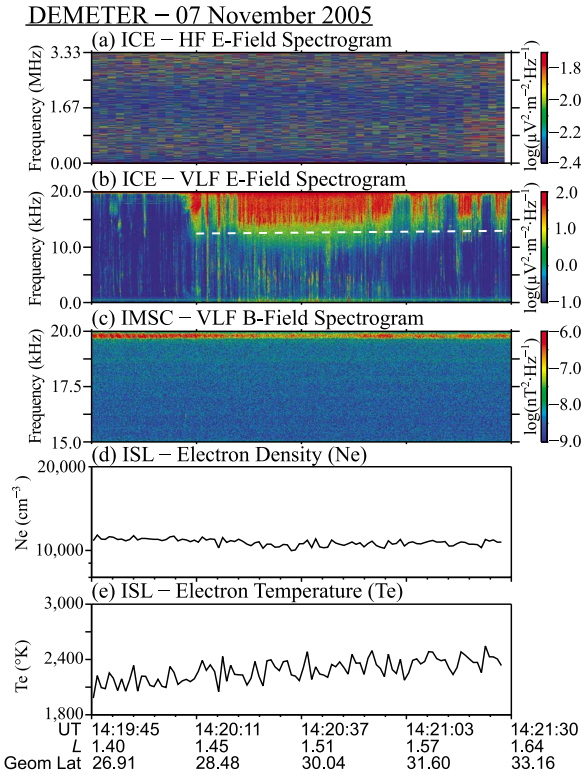

Figure 3. Observations above NWC conjugate point: (a) spectrogram of impulsive MF signals; (b) spectrogram of an E field component of VLF plasma waves; (c) spectrogram of a B field component of VLF plasma waves; (d) local electron density; (e) local electron temperature. The position of closest approach to the NWC conjugate reference point is reached at 1419:19 UT. The magnetic longitude is ≃183°E. DEMETER altitude is ≃708 km.

time interval, T_e exhibits a maximum increase of ≃15%. If Figures 2d and 2e are compared with Figures 1d and 1e, it is clear that the ionospheric effects produced by NAA at 700 km altitude are modest when compared to the effects produced by NWC, and that the spatial form of the perturbations are dissimilar. Nevertheless Figure 2a shows that lightning generated impulsive MF signals can still be observed within the heated region, suggesting that the changes in N_e produced by NAA are still sufficient to allow the MF waves to penetrate the F region.

2.3. Ionospheric Heating Effects in the NWC and NAA Conjugate Regions

[11] Figure 3 shows representative DEMETER plasma wave and N_e and T_e observations during a pass over the region magnetically conjugate to the NWC VLF transmitter on 7 November 2005, from 1419:45 to 1421:30 UT. The format is the same as in Figures 1 and 2. Figure 3b shows a high resolution (burst mode) 0 to 20 kHz spectrogram of a component of the observed E field of plasma waves. The spectra include the NWC signal at 19.8 kHz plus a band of plasma waves (red color) located below the NWC signal frequency which are observed over the approximate time interval 1420:10 to 1421:30 UT and occupy the approximate frequency range: 13 to 20 kHz. Since Figure 3c shows no detectible B field for these waves, it is clear that they are a QE wave band. The QE band was observed on all 50 passes, and appears to consist predominantly of numerous relatively intense impulsive signals extending in frequency from $\simeq f_{lhr}$ to 20 kHz. In Figure 3b the calculated value of f_{lhr} is shown by a white dashed line.

[12] Comparison of Figure 1b with Figure 3b suggests that the two bands of QE waves are quite similar in bandwidth, but the intensity of the QE waves over NWC is ≃10 dB higher than those in the conjugate region. The QE wave band in the NWC conjugate region extends over a larger distance (600 km) and occurs at higher L shells (1.4–1.6) than the QE wave band over NWC. Thus the QE band in the conjugate region is not merely the field line mapping of the QE band over NWC into the conjugate region.

[13] Figures 3d and 3e show that there are no large changes in N_e and T_e during the time period over which the band of QE plasma waves is observed, the fluctuations in N_e being less than 10%. This holds true for the 50 cases we have examined. Thus the large changes in N_e and T_e observed over NWC do not appear to extend into the conjugate region. However, there is always a band of ELF QE turbulence present when the QE wave band is observed in the conjugate region, as illustrated in Figure 4. A QE band of ELF turbulence is also always present in the heated regions over NWC and NAA. This form of turbulence has been associated with small scale plasma density irregularities [*Cerisier et al.*, 1985].

[14] From Figure 3a, it can be seen that no significant MF whistler impulses are present in the conjugate region. This supports the suggestion that significant plasma density irregularities are necessary for these impulses to reach 700 km altitude [*Parrot et al.*, 2009]. DEMETER observations over the NAA conjugate region show no effects such as those seen in Figure 3.

3. Discussion

[15] It does not appear likely that the heating effects shown in Figures 1 and 2 have their origin in the D-region. For example, *Rodriguez and Inan* [1994] found that a 1 MW VLF transmitter could produce at most a 300° rise in T_e and a 26% decrease in N_e over the altitude range 70–90 km above the transmitter. These localized D-region changes are smaller than those observed at 700 km altitude by DEMETER. Thus the heating effects observed on DEMETER most likely occur somewhere between the E-region and 700 km altitude. Furthermore, the presence of MF whistler components above

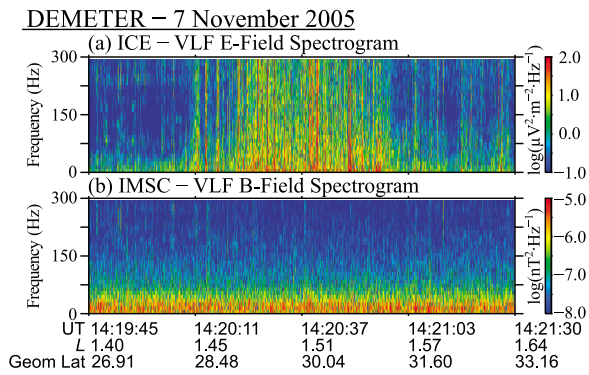

Figure 4. Spectrograms of ELF turbulence above NWC conjugate point: (a) E field; (b) B field.

NWC and NAA suggests that the heated region extends below the F region. The mechanism which produces this heating is open to question, but the QE wave bands and the ELF turbulence observed over the NWC and NAA transmitters may be involved in the heating process. For example, *Bell et al.* [1993] discuss a similar system in which ionospheric ions are energized by impulsive QE waves excited by lightning-generated whistlers above thunderstorm cells. Whatever the cause, the heating shown in Figures 1 and 2 represents an additional power loss for the transmitter signals which will contribute to the pervasive wave intensity deficit for VLF transmitter signals recently reported by *Starks et al.* [2009].

[16] The data presented in Figures 1 and 3 suggest that heating effects due to NWC are far-reaching and extend along B_o into the conjugate hemisphere where they are expressed in part as small scale plasma density fluctuations. However this does not appear to be the case for NAA. Furthermore, comparing Figure 1 with Figure 2, it is apparent that the ionospheric heating produced by the VLF waves from the NWC transmitter results in much larger changes in N_e and T_e at 700 km altitude than those produced by the VLF waves from the NAA transmitter.

[17] In spite of this fact, comparison of Figures 1a and 2a shows that the whistler MF impulses generally observed over NAA can be as numerous and intense as those generally observed over NWC. One possible reason for this similarity is the fact that at the latitude of NAA the local values of N_e at 700 km altitude are generally smaller than those over NWC by at least a factor of two. If this scaling also applies down to the F region, then less heating would be required to allow the MF impulses to penetrate the F region.

[18] The origin of the QE wave bands that appear in Figures 1b and 2b becomes clear when high resolution burst mode data is examined. Burst mode data was not routinely acquired during orbits directly over NWC and NAA, and our 50 example data set for NWC and NAA contains no burst mode data. However burst mode data was occasionally acquired on orbits whose distance of closest approach from NWC and NAA was in range of 200–400 km. At these distances DEMETER was still within the heated region. The wave data acquired on these orbits closely resembles that shown in Figure 3b.

[19] In Figure 3b, the intense impulsive signals appear to be QE waves excited by lightning-generated EM whistler impulses as the EM impulses experience linear mode coupling [*Bell and Ngo*, 1990] as they propagate upward through small scale plasma density irregularities, whose presence is suggested by the ELF turbulence shown in Figure 4. This turbulence is always present in the NWC conjugate region wherever the QE wave band is observed. This suggests that the turbulence is directly related to the heating that takes place over NWC.

[20] Based on the DEMETER plasma wave burst mode data acquired at ranges of 200–400 km and its close resemblance to Figure 3b, it appears that the QE wave bands shown in Figures 1b and 2b also consist of impulsive QE waves excited by lightning-generated EM whistler impulses as they propagate upward through small scale plasma density irregularities. According to the model of *Bell and Ngo* [1990], these QE waves should exist at all $f \geq f_{lhr}$, similar to what is seen in the data.

[21] Alternative mechanisms for producing the QE wave band over NWC have recently been proposed by *Mishin et al.* [2010], who suggest that the QE wave band may be generated through nonlinear parametric interactions driven by the input VLF transmitter signals. In this model the parametric instabilities could eventually generate QE waves whose true frequencies would lie between f_{lhr} and the transmitter frequency. The QE wave band example shown in *Mishin et al.*'s [2010] paper is low resolution data similar to Figure 1b which does not show the impulsive nature of the QE waves. It is not clear how *Mishin et al.*'s [2010] model can be applied to the case of impulsive input waves.

[22] **Acknowledgments.** The Stanford University STAR Laboratory is a Guest Investigator of the French micro-satellite DEMETER operated by CNES (Centre National d'Etudes Spatiales). The Stanford authors were supported by the Department of the Air Force, under grant F49620-03-1-0338-P00002 and contract F19628-03-C-0059-P00002.

[23] The Editor thanks Frantisek Nemec and an anonymous reviewer for their assistance evaluating this paper.

References

Barr, R., and P. Stubbe (1992), VLF heating of the lower ionosphere: Variation with magnetic latitude and electron density profile, *Geophys. Res. Lett.*, *19*, 1747–1750.

Bell, T. F., and H. D. Ngo (1990), Electrostatic lower hybrid waves excited by electromagnetic whistler mode waves scattering from planar magnetic-field-aligned plasma density irregularities, *J. Geophys. Res.*, *95*, 149–172.

Bell, T. F., R. A. Helliwell, U. S. Inan, and D. S. Lauben (1993), The heating of suprathermal ions above thunderstorm cells, *Geophys. Res. Lett.*, *20*, 1991–1994.

Cerisier, J. C., J. J. Berthelier, and C. Beghin (1985), Unstable density gradients in the high-latitude ionosphere, *Radio Sci.*, *20*(4), 755–761.

Galejs, J. (1972), Ionospheric interaction of VLF radio waves, *J. Atmos. Terr. Phys.*, *34*, 421–436.

Inan, U. S. (1990), VLF heating of the lower ionosphere, *Geophys. Res. Lett.*, *17*, 729–732.

Inan, U. S., J. V. Rodriguez, S. Lev-Tov, and J. Oh (1992), Ionospheric modification with a VLF transmitter, *Geophys. Res. Lett.*, *19*, 2071–2074.

Mishin, E. V., M. J. Starks, G. P. Ginet, and R. A. Quinn (2010), Nonlinear VLF effects in the topside ionosphere, *Geophys. Res. Lett.*, *37*, L04101, doi:10.1029/2009GL042010.

Parrot, M. (2006), Special issue of planetary and space science 'DEMETER,' *Planet. Space Sci.*, *54*, 411–412.

Parrot, M., U. S. Inan, N. G. Lehtinen, and J. L. Pinçon (2009), Penetration of lightning MF signals to the upper ionosphere over VLF ground-based transmitters, *J. Geophys. Res.*, *114*, A12318, doi:10.1029/2009JA014598.

Parrot, M., J. A. Sauvaud, J. J. Berthelier, and J. P. Lebreton (2007), First in-situ observations of strong ionospheric perturbations generated by a powerful VLF ground-based transmitter, *Geophys. Res. Lett.*, *34*, L11111, doi:10.1029/2007GL029368.

Rodriguez, J. V., and U. S. Inan (1994), Electron density changes in the nighttime *D* region due to heating by very-low-frequency transmitters, *Geophys. Res. Lett.*, *21*, 93–96.

Rodriguez, J., U. Inan, and T. Bell (1994), Heating of the nighttime *D* region by very low frequency transmitters, *J. Geophys. Res.*, *99*, 23,329–23,338.

Starks, M. J., T. F. Bell, R. A. Quinn, U. S. Inan, D. Piddyachiy, and M. Parrot (2009), Modeling of Doppler-shifted terrestrial VLF transmitter signals observed by DEMETER, *Geophys. Res. Lett.*, *36*, L12103, doi:10.1029/2009GL038511.

Taranenko, Y. N., U. S. Inan, and T. F. Bell (1992), VLF-HF heating of the lower ionosphere and ELF wave generation, *Geophys. Res. Lett.*, *19*, 61–64.

T. F. Bell, K. Graf, U. S. Inan, and D. Piddyachiy, STAR Laboratory, Stanford University, 350 Serra Mall, Stanford, CA 94305, USA. (bell@nova.stanford.edu)

M. Parrot, LPC2E, CNRS, 3A Avenue de la Recherche Scientifique, F-45071 Orleans CEDEX 2, France.